High-Rate, Long-Life Ni–Sn Nanostructured Electrodes for Lithium-Ion Batteries

Jusef Hassoun, Stefania Panero, Patrice Simon, Pierre-Louis Taberna, Bruno Scrosati

DOI: 10.1002/adma.200602035

High-Rate, Long-Life Ni–Sn Nanostructured Electrodes for Lithium-Ion Batteries**

By *Jusef Hassoun*, *Stefania Panero*, *Patrice Simon*, *Pierre Louis Taberna*, and *Bruno Scrosati**

Lithium metal (LiM) alloys, owing to their intrinsic high specific capacity, are considered to be very appealing negative electrodes that may be exploited for the replacement of conventional graphite in advanced design, lithium-ion batteries. LiM alloys, however, undergo large volume expansion and contraction during the charge–discharge cycling, which induces mechanical disintegration that results in very poor cycle life.

Large research efforts are presently devoted to overcome this problem with the final goal of making these appealing materials for the effective use as innovative, high-performance electrodes.[1–5] A promising approach is that of moving to M_1M_2 intermetallics where the electrochemical process in a lithium cell involves the displacement of one metal, e.g., M_2, which forms the desired lithium alloy, LiM_2, while the other metal, M_1, acts as an electrochemically inactive matrix to buffer the volume variations during the alloying process. Among others, tin-based intermetallics have received particular attention due to their specific properties, which combine high charge storage with low cost.[6] Various compositions have been investigated to identify the ones that are the most promising in terms of battery applications. The Ni_3Sn_4 phase is one of these.[7–10]

The electrochemical process for this Ni_3Sn_4 intermetallic is expected to evolve by a first activation step:

$$Ni_3Sn_4 + 17.6Li^+ + 17.6e^- \rightarrow 4Li_{4.4}Sn + 3Ni \quad (1)$$

followed by the main, reversible electrochemical process:

$$Li_{4.4}Sn \rightarrow Sn + 4.4\,Li^+ + 4.4e^-(\text{charge}) \quad (2)$$

$$Sn + 4.4\,Li^+ + 4.4e^- \rightarrow Li_{4.4}Sn(\text{discharge}) \quad (3)$$

While the first step is irreversible, the following ones are in principle reversible and represent the steady-state electrochemical operation of the electrode to which is associated a total, theoretical capacity of 993 $mA\,h\,g^{-1}$, calculated with respect to the mass of tin. The capacity retention of the Ni_3Sn_4 intermetallic electrode, although improved with respect to that of plain Sn electrodes, is not totally satisfactory with prolonged cycling.[7–11]

It is now recognized that an efficient way of improving the electrochemical response of lithium-alloy electrodes is that of optimizing their morphology, especially in terms of particle size and interparticle space.[12] This may be obtained by the refinement of preparation methods, aiming to lead to optimized electrode configurations.

In previous work we reported the behavior of Ni_3Sn_4 intermetallic electrodes prepared by electrodeposition onto a flat Cu electrode substrate.[13] By varying the conditions of the electrodeposition process, we could control the final electrode morphology and accordingly, the electrode behavior. We showed that these electrodeposited Ni_3Sn_4 electrodes could provide a stable capacity of 300 $mA\,h\,g^{-1}$ for a total of 70 high-rate (1C), charge–discharge cycles.[13] Although of interest, this result is still not satisfactory for allowing the use of the Ni_3Sn_4 electrode in batteries addressed to demanding applications such as hybrid vehicle or renewable-energy storage.

In this paper, we report a revolutionary, new type of nanoarchitectured configuration that results in electrodes that have very high rate capability and excellent capacity retention. The new electrode configuration designed in this work was prepared by a template synthesis procedure that initially involved the formation of a nanoarchitectured Cu current collector. This was obtained by growing a 3D array of Cu nanorods onto a Cu foil by electrodeposition through a porous alumina membrane that was subsequently dissolved. Figure 1 illustrates side and top views of this Cu nanopillar current collector. The scanning electron microscopy (SEM) image clearly shows the uniformly distributed Cu rods of about 200 nm diameter, as defined by the pore size of the alumina template, emerging from the Cu surface below. The synthesis was then completed by coating the above-described Cu nanorod array with Ni_3Sn_4 particles. Two different electrode samples were prepared and named NiSn-1 and NiSn-2 (see the Experimental section and Table 1 for sample identification).

Figure 2 shows X-ray diffraction (XRD) patterns of the two electrode samples. With the exception of the reflections of the support, the peaks are attributed to the Ni_3Sn_4 phase. In fact, these peaks match those reported for Ni_3Sn_4 prepared by using electrodeposition.[8,13,14] Both samples show a rather amorphous feature; however, the few peaks in the NiSn-2

[*] Prof. B. Scrosati, Dr. J. Hassoun, Prof. S. Panero
Department of Chemistry, University of Rome "La Sapienza"
P.le Aldo Moro 5, 00185 Rome (Italy)
E-mail: bruno.scrosati@uniroma1.it
Prof. P. Simon, Dr. P. L. Taberna
CIRIMAT-UMR 5085—Université Paul Sabatier
route de Narbonne, 31062 Toulouse, Cedex 4 (France)

[**] This work has been carried out with the financial support of the European Network of Excellence ALISTORE and of the Italian Ministry of University and Research under a PRIN 2005 project. The authors wish to thank the Scanning Electron Microscopy Laboratory of the Department of General Biology of the University of Rome "La Sapienza" for the help in the SEM investigation.

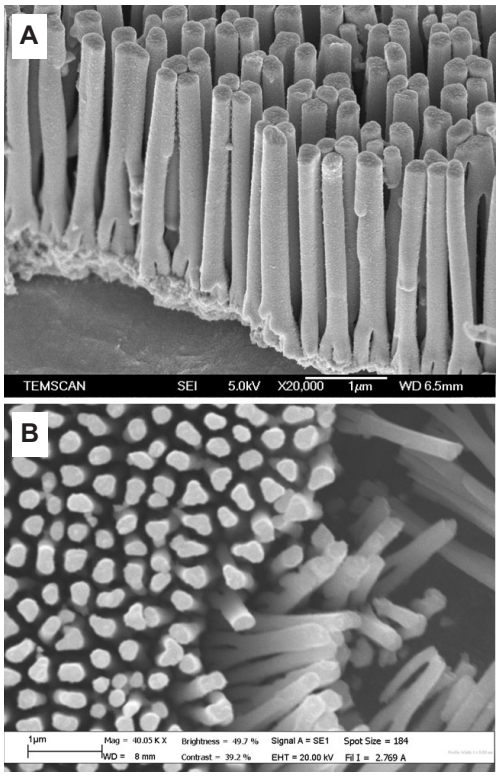

Figure 1. SEM image of A) side and B) top views of the Cu nanorods current collector used as a support for the electrodeposition of the intermetallic samples.

Table 1. Conditions for the electrodeposition of the Ni_3Sn_4 samples prepared in this work.

Sample	Electrodeposition current [mA cm^{-2}]	Electrodeposition time [min]	Electrodeposition capacity [C]
NiSn-1	6.0	5	1.8
NiSn-2	6.0	1.25	0.45

sample pattern are smaller than those observed for the NiSn-1 sample, this probably being associated with the different amount of electrodeposited material that is smaller in NiSn-2 than in NiSn-1, see Table 1. Apart from this small difference, the two XRD patterns are rather similar.

The morphology of the two samples is however quite different. Figure 3 shows the top view of the two samples. By comparison with the morphology of the pristine Cu nanostructured current collector, see Figure 1, one notices that in sample NiSn-2 (Fig. 3B), the Ni_3Sn_4 nanoparticles (of the order of 50 nm) are uniformly deposited on the surface of the Cu nanorods without any coalescence between them. In contrast, in the case of sample NiSn-1, formed by extending the coating to a higher amount (see Table 1), the degree of coverage increased up to the formation of a continuous film onto the nanopillar substrate (Fig. 3A).

This difference in morphology is quite convenient for comparing the electrochemical behavior of the nanostructured electrode (sample NiSn-2, Fig. 3B) versus that of the bulk electrode (sample NiSn-1, Fig. 3A) over flat surface configurations. Sample NiSn-1, which was intentionally prepared with a compact, flat surface, is expected to undergo the well-known cycling difficulties associated with the mechanical disintegration resulting from volume stresses. This is indeed the case as demonstrated in Figure 4, which reports the electrochemical response of this sample, NiSn-1, cycled in a galvanostatic mode in a lithium cell. The electrode operates in charge and discharge with the voltage profile expected on the basis of processes (2) and (3), see Figure 4B. The reversible initial capacity delivery is of the order of 400 mA h g^{-1}, that is, about 40 % of the theoretical value, see Figure 4A. However, a dramatic capacity decay is observed near the 50th cycle, suggesting the occurrence of electrode failure. Indeed, Figure 4C, which reports the SEM image of this NiSn-1 electrode after the cycling test, clearly evidences the formation of cracks on the electrode surface, as fatally expected for compact structures.

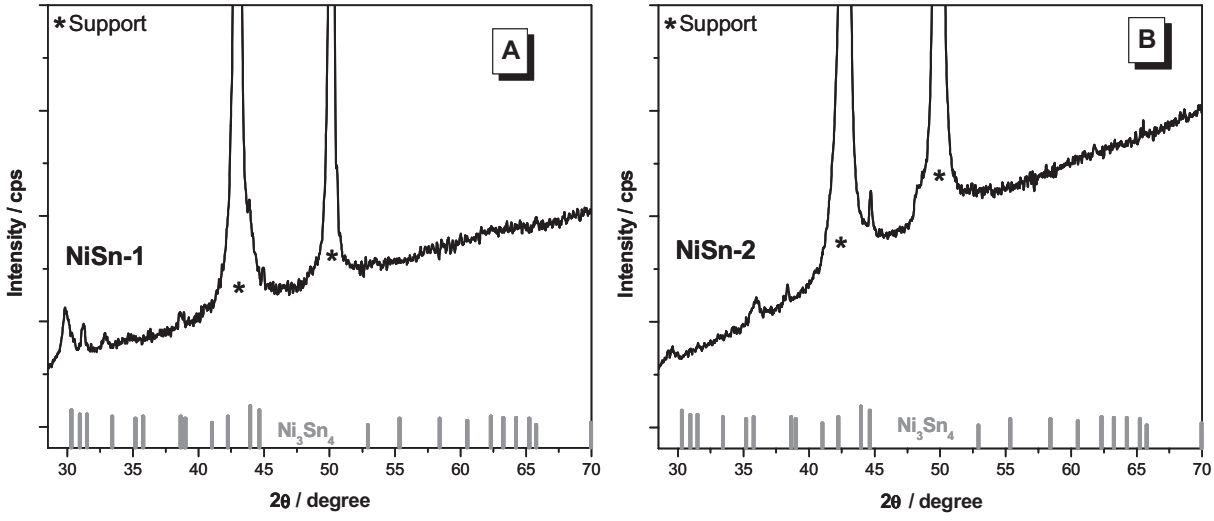

Figure 2. XRD patterns of the A) NiSn-1 and B) NiSn-2 samples investigated in this work. For samples' identification see Table 1.

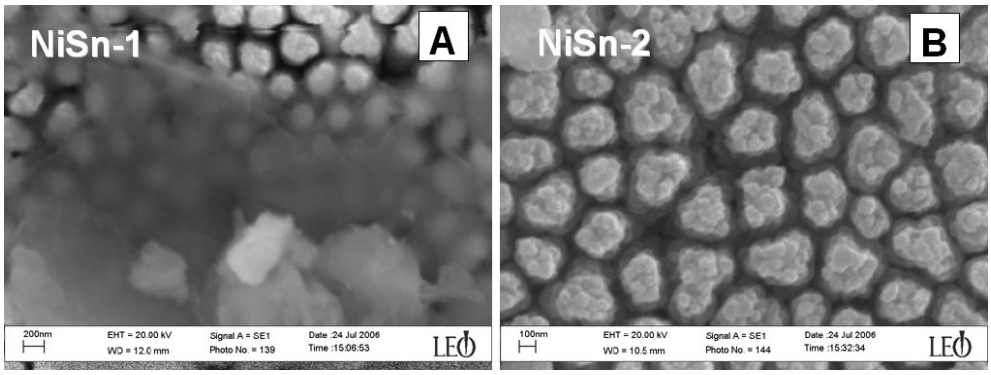

Figure 3. SEM images of the A) NiSn-1 and B) NiSn-2 samples investigated in this work. For samples' identification see Table 1.

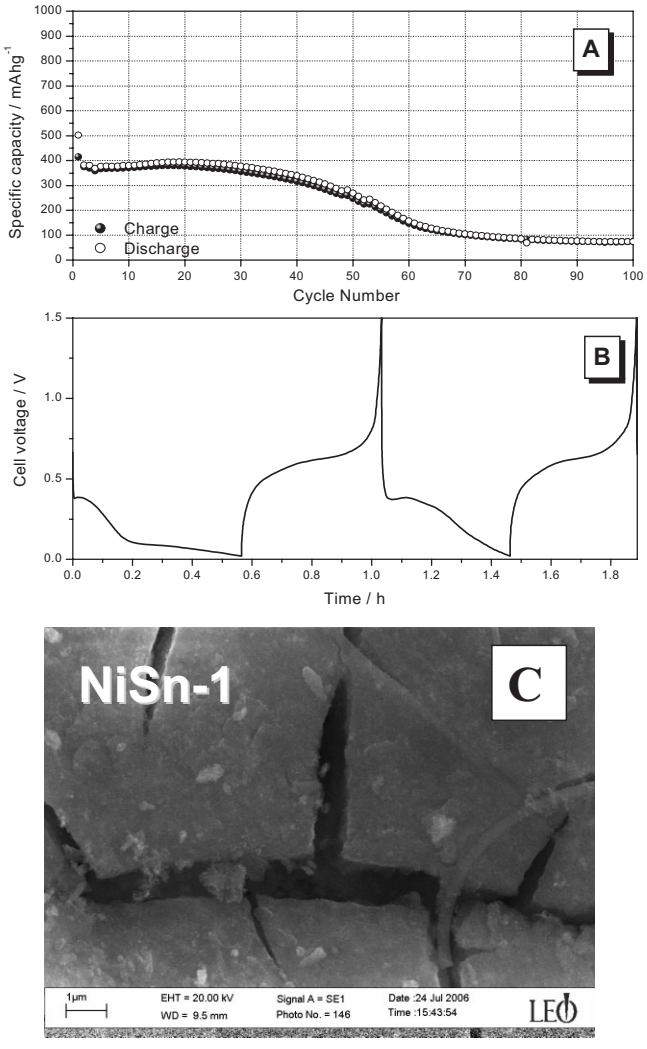

Figure 4. A) Capacity delivered upon cycling and B) voltage profiles of the first two cycles of sample NiSn-1 used as an electrode in a lithium cell. C) SEM image of the electrode after the cycling test. Cycling was between 0.02 and 1.5 V at a rate of ca. 0.8C. For samples' identification see Table 1.

Quite different is the response of the nanostructured electrode NiSn-2. The charge–discharge voltage profiles are smoother than in the previous case (Fig. 5B), and more importantly, the capacity delivery is kept at high values for 200 cycles, with no sign of decay (Fig. 5A). Indeed, SEM examination of this NiSn-2 electrode after the cycling test does not show appreciable variation of the initial morphology (compare Fig. 5C with Fig. 3B). Obviously, the Ni_3Sn_4 alloy deposited on the Cu nanorods experiences the same internal stress as that of the Ni_3Sn_4 alloy deposited on a flat surface. In the case of the nanostructured electrode, however, the volume variations upon cycling are effectively buffered by the large free volume between the pillars, thus giving to the electrode the observed excellent capacity retention.

Owing to the small size of the Ni_3Sn_4 particles, which are of the order of 50 nm, the NiSn-2 electrode is expected to have a high rate capability. This is indeed demonstrated in Figure 6, which shows the cycling response at progressively increasing rates. Even at rates as high as 10C, the electrode is capable of operating at a good fraction of its capacity, which is a behavior, to our knowledge, rarely seen for common LiM electrodes. By returning to the initial rate of 0.8C, the electrode resumes the original capacity of about 500 mA h g^{-1}, and continues to operate with a stable cycling response.

In summary, this work describes Ni_3Sn_4 intermetallic electrodes prepared into a new, revolutionary nanostructure obtained by electrodeposition on a nanoarchitectured Cu substrate. This particular nanostructure, first proposed by Taberna et al. for the preparation of iron oxide electrodes,[15] appears particularly suitable for LiM alloy electrodes, as it is effectively able to accommodate the volume variations occurring during cycling in a lithium cell, this resulting in high-rate electrodes with excellent capacity retention.

Tests in lithium cells show that the nanostructured Ni_3Sn_4 electrodes cycle with a capacity of the order of 500 mA h g^{-1} with no decay over 200 cycles. In addition, these electrodes may operate at rates as high as 10C while still delivering 20 % of their theoretical capacity. These are performances rarely reported for LiM alloy electrodes, and thus, we think that the results reported in this work may open the route for using these electrodes in new-design, high-performance lithium-ion batteries. This expectation is presently under test in our laboratories.

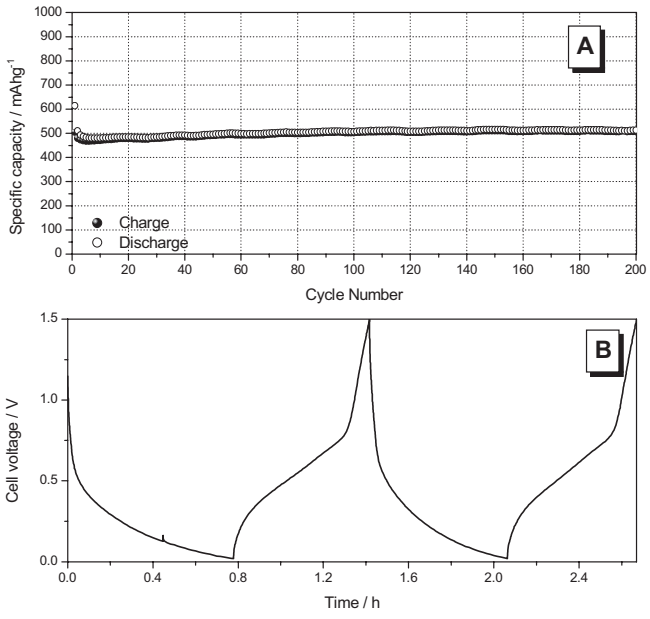

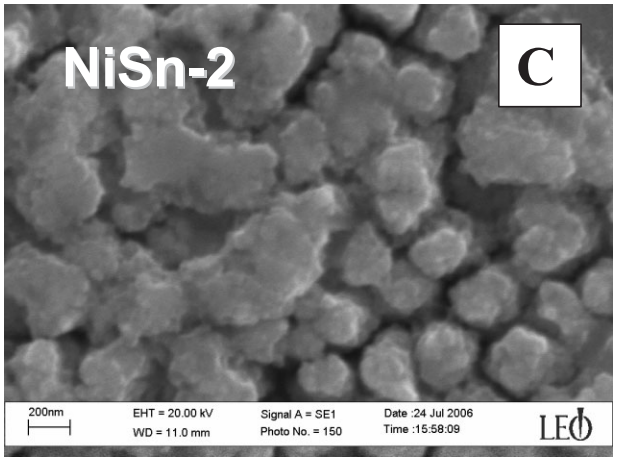

Figure 5. A) Capacity delivered upon cycling and B) voltage profiles of the first two cycles of sample NiSn-2 used as electrode in a lithium cell. C) SEM image of the electrode after the cycling test. The cycling test was run between 0.02 and 1.5 V at a rate of ca. 0.8C. For samples' identification see Table 1.

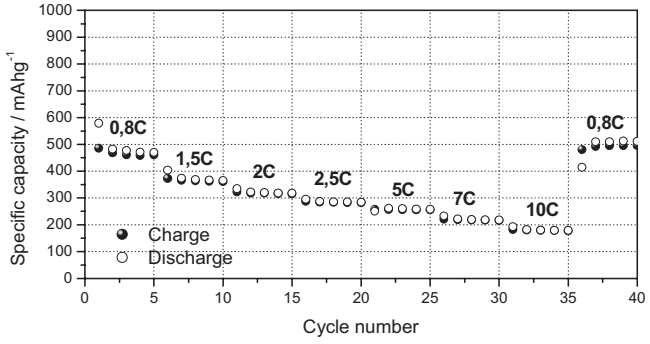

Figure 6. Capacity delivered upon cycling at various rates by sample NiSn-2 cycled between 0.02 and 1.5 V in a lithium cell.

Experimental

The Ni_3Sn_4 electrodes were obtained following a template synthesis procedure designed by Taberna et al. for the preparation of nanostructured iron oxide electrodes [15]. Basically, this procedure involves the use of a nanoarchitectured Cu current collector prepared by growing a 3D array of Cu nanorods onto a Cu foil by using electrodeposition through a porous alumina membrane that it is subsequently dissolved [15]. The synthesis was then completed by coating the above-described Cu nanorod array with Ni_3Sn_4 particles. This was achieved by electrodeposition in a two-electrode glass cell. An aqueous solution, formed by $NiCl_2$ 0.075 M, $SnCl_2$ 0.175 M, $K_4P_2O_7$ 0.5 M, glycine 0.125 M, and NH_4OH 5 ml L^{-1} [8,13] was used as the electrodeposition solution and a Pt foil as the counter electrode. The electrodeposition current and time conditions were monitored using a Maccor Series 4000 Battery Test System. We used this procedure to prepare two different electrode samples by varying the electrodeposition conditions. The first sample, coded as NiSn-1, was deposited using a 1.8 C cm^{-2} capacity, while the second, coded NiSn-2, was 25 % less coated than the first, by using 0.45 C cm^{-2} capacity. Table 1 summarizes the electrodeposition protocols for the two samples.

The structure of the samples was determined by XRD, using a Rigaku X-ray diffractometer miniflex and their morphology was observed by using SEM using SEM Leo EVO 40 instrumentation.

The electrochemical response of the samples was tested in cells based on the following sequence: i) an electrode formed by the given Ni_3Sn_4 sample electrodeposited onto the Cu nanostructured current collector, ii) a 1 M $LiPF_6$ electrolyte solution in an ethylene carbonate/dimethyl carbonate 1:1 (Merck Battery Grade) mixture soaked into a Whatman separator and iii) a Li foil counter electrode. The cells were cycled at room temperature at a 0.8C rate and between a 0.02–1.5 V voltage limit. The delivered capacity is quoted with respect to the mass of the electrode, that is, the mass of the alloy. The electrochemical response of the cells was tested under constant charge–discharge cycles using a Maccor Series 4000 Battery Test System.

[1] J. Yang, Y. Takeda, N. Imanischi, J. Y. Xie, O. Yamamoto, *Solid State Ionics* **2000**, *133*, 189.
[2] D. Larcher, L. Y. Beaulieu, O. Mao, A. E. George, J. R. Dahn, *J. Electrochem. Soc.* **2000**, *147*, 1703.
[3] R. Benedek, M. M. Thackeray, *J. Power Sources* **2002**, *147*, 406.
[4] C. S. Johnson, J. T. Vaughey, M. M. Thackeray, T. Sarakonsri, S. A. Hackney, L. Fransson, K. Edström, J. O. Thomas, *Electrochem. Commun.* **2002**, *2*, 595.
[5] Z. Chen, V. Chevrier, L. Christensen, J. R. Dahn, *Electrochem. Solid-State Lett.* **2004**, *7*, A310.
[6] M. Winter, J. O. Besenhard, *Electrochim. Acta* **1999**, *45*, 31.
[7] H.-Y. Lee, S.-W. Jang, S.-M. Lee, S.-J. Lee, H.-K. Baik, *J. Power Sources* **2002**, *112*, 8.
[8] H. Mukaibo, T. Sumi, T. Yokoshima, T. Momma, T. Osaka, *Electrochem. Solid-State Lett.* **2003**, *6*, A218.
[9] Q. F. Dong, C. Z. Wu, M. G. Jin, Z. C. Huang, M. S. Zheng, J. K. You, Z. G. Lin, *Solid State Ionics* **2004**, *167*, 49.
[10] I. Amadei, S. Panero, B. Scrosati, G. Cocco, L. Schiffini, *J. Power Sources* **2005**, *143*, 227.
[11] J. Hassoun, S. Panero, P. Reale, B. Scrosati, *J. Electrochem. Sci.* **2006**, *1*, 110.
[12] A. Aricò, P. Bruce, B. Scrosati, J.-M. Tarascon, W. van Schalkwijk, *Nat. Mater.* **2005**, *4*, 366.
[13] J. Hassoun, S. Panero, B. Scrosati, *J. Power Sources* **2006**, *160*, 1136.
[14] T. Watanabe, T. Hirose, K. Arai, M. Chikazawa, *Nippon Kinzoku Gakkaishi* **1999**, *63*, 496.
[15] P. L. Taberna, S. Mitra, P. Piozot, P. Simon, J. M. Tarascon, *Nat. Mater.* **2006**, *5*, 567.